

# LARGE-SCALE STRUCTURE OF THE DOLDRUMS MULTI-FAULT TRANSFORM SYSTEM (7-8°N EQUATORIAL ATLANTIC): PRELIMINARY RESULTS FROM THE 45<sup>th</sup> EXPEDITION OF THE *R/V A.N. STRAKHOV*

Sergey G. Skolotnev\*, Alessio Sanfilippo\*\*,✉, Alexander Peyve A.\*, Filippo Muccini\*\*\*, Sergey Yu. Sokolov\*, Camilla Sani\*\*, Kseniia O. Dobroliubova\*, Carlotta Ferrando°, Nikolai P. Chamov\*, Camilla Palmiotto°, Alexey N. Pertsev°, Enrico Bonatti°, Marco Cuffaro°, Anastasiya C. Gryaznova\*\*, Konstantin N. Sholukhov°, Artem S. Bich\*\* and Marco Ligi°

\* *Geological Institute, Russian Academy of Sciences, Moscow, Russia.*

\*\* *Dipartimento di Scienze della Terra e dell'Ambiente, Università di Pavia, Italy.*

\*\*\* *Istituto Nazionale di Geofisica e Vulcanologia, Roma, Italy.*

° *Centre de Recherche Petrographique et Geochemique, CNRS, Vandoeuvre - Les-Nancy, France.*

°° *Istituto di Scienze Marine, CNR, Bologna, Italy.*

°°° *Institute of Ore Deposits, Petrography, Mineralogy and Geochemistry, Russian Academy of Sciences, Moscow, Russia.*

• *Istituto di Geologia Ambientale e Geoingegneria, CNR, c/o Dipartimento Scienze della Terra, Sapienza Università Roma, Italy.*

•• *Vernadsky Institute of Geochemistry and Analytical Chemistry, Russian Academy of Sciences, Moscow, Russia.*

••• *Polar Marine Geological Prospecting Expedition, Lomonosov, Russia.*

✉ *Corresponding author, e-mail: alessio.sanfilippo@unipv.it*

**Keywords:** *oceanic transforms; peridotite; gabbro; basalt; mantle exhumation; Mid Atlantic ridge.*

## ABSTRACT

The Equatorial portion of the Mid Atlantic Ridge is displaced by a series of large offset oceanic transforms, also called “megatransforms”. These transform domains are characterized by a wide zone of deformation that may include different conjugated fault systems and intra-transform spreading centers (ITRs). Among these megatransforms, the Doldrums system (7-8°N) is arguably the less studied, although it may be considered the most magmatically active. New geophysical data and rock samples were recently collected during the 45<sup>th</sup> expedition of the *R/V Akademik Nikolaj Strakhov*. Preliminary cruise results allow to reconstruct the large-scale structure and the tectonic evolution of this poorly-known feature of the Equatorial Atlantic. Swath bathymetry data, coupled with extensive dredging, were collected along the entire megatransform domain, covering an area of approximately 29,000 km<sup>2</sup>. The new data clearly indicate that the Doldrums is an extremely complex transform system that includes 4 active ITRs bounded by 5 fracture zones. Although the axial depth decreases toward the central part of the system, recent volcanism is significantly more abundant in the central ITRs when compared to that of the peripheral ITRs. Our preliminary interpretation is that a region of intense mantle melting is located in the central part of the Doldrums system as consequence of either a general transtensive regime or the occurrence of a more fertile mantle domain. Large regions of basement exposure characterize the transform valleys and the ridge-transform intersections. We speculate that different mechanisms may be responsible for the exposure of basement rocks. These include the uplift of slivers of oceanic lithosphere by tectonic tilting (median and transverse ridges formation), the denudation of deformed gabbro and peridotite by detachment faulting at inner corner highs, and the exposure of deep-seated rocks at the footwall of high-angle normal faults at the intersection of mid-ocean ridges with transform valleys.

## INTRODUCTION

Our knowledge of the geodynamic evolution of mid-ocean ridges (MOR) relies on the idea that different sectors of an ocean ridge are separated by discontinuities oriented parallel to the direction of seafloor spreading. These are tectonically active features corresponding to oceanic transform boundaries. In a classical idea, an oceanic transform consists of a single narrow (a few km) strike-slip zone offsetting two mid-ocean ridge segments (Wilson, 1965). However, some oceanic transform domains can be locally characterized by a broad (> 100 km) and complex multi-fault zone of deformation similar to that of some continental strike-slip systems. These domains have exceptionally long age offset (up to 50 Ma), and are regarded as “megatransforms” or megatransform system (MTS) (Ligi et al., 2002). Examples of these MTS are those displacing the equatorial portion of the Mid-Atlantic Ridge (MAR) such as Romanche and St. Paul, or Andrew Bain in the South West Indian Ridge. These long transform zones display particularly complex morphologies, reflecting their evolution through time. In particular, the relative motion along MTS involves the deformation of extraordinarily

thick and cold lithosphere. Following this rationale, Ligi et al. (2002) proposed that the extreme thickness of the lithosphere determines the unusual width and complex geometry of MTS. They found that long age-offset (> 30 Ma) faults produce two major symmetrical faults joining the two ridge segments, with a lens-shaped, complex and wide deformed area in between. The composite plate boundary at these locations strongly affects the main processes building the oceanic lithosphere, such as fluid circulation, mantle exhumation, mantle melting and magmatism (see also Sclater et al., 2005).

An archetypical example of megatransform is the Romanche fracture zone (FZ), where the morpho-bathymetry shows that the entire transform domain is deeper than MOR average bathymetry and that the lens-shaped deformed region is clearly bounded by two major fault systems, likely active at alternate periods (Ligi et al., 2002). The eastern Romanche ridge-transform intersection (RTI) clearly shows the effects of the lateral cooling due to the thick and cold lithosphere facing the warmer ridge segment tip: the style of spreading changes from normal to oblique and magmatism is reduced, or even absent, when approaching the transform. As a consequence, the accretionary process changes from a symmetric

rift valley at the centre of the segment to oblique asymmetric smooth-seafloor-like structures (Cannat et al., 2006) associated to a discontinuous gabbroic layer next to the RTI. Detailed geological data on the variability of volcanism in the region agree with this idea showing a general decrease in the degree of partial melting approaching the RTI (Ligi et al., 2005). Modelling of the subridge thermal structure suggests that the reason for the constipated magma production is basically due to a decrease in the along-axis thermal gradient (Bonatti et al., 1996a; 2001). Such a strong change in thermal conditions may result in a dramatic reduction of the melting region, possibly reflected in the style of seafloor morphologies. For this reason, the MAR equatorial portion has been interpreted as a major “thermal minimum”, partly due to the “cold edge” effect related to the large offset transforms segmenting the ridge system (White et al., 1984; Schilling et al., 1995; Bonatti, 1996a).

North of the Romanche, the St. Paul system consists of four transform faults separated by three ITRs, offsetting the MAR by ~ 580 km and displaying a total age contrast of 40 Ma (Hekinian et al., 2000). The occurrence of these ITRs is counterintuitive, due to the high lithospheric thickness expected in the central portion of a megatransform. Hence, either active mantle upwelling or changes in plate motions towards a transtensive regime can be the driving forces for the opening of ITRs (Bonatti, 1978; Maia et al., 2016). North of St. Paul, the Doldrums MTS offsets the MAR axis for about 630 km. Although this system is arguably the most complex,

including 4 ITRs and 5 transform faults, detailed bathymetric and sample analyses are confined to the westernmost sector (Fig. 1). Yet, there are few data so far on the basalts and basement rocks from this region, making the origin of this long-offset transform domain poorly constrained.

Here we report new geophysical and lithological data on a recent survey conducted during cruise S45 of the *R/V Akademik Nikolaj Strakhov* (November 2019). Multibeam data acquisition was carried out along the entire megatransform domain, covering the four ITRs for an area of approximately 29,000 km<sup>2</sup>. Along with a preliminary characterization of > 1300 kg of rocks from 12 dredges, the new data are here used to interpret the evolution of this poorly known MTS.

### GEOLOGICAL SETTING OF THE DOLDRUMS MEGATRANSFORM SYSTEM

Located in the northern portion of the Equatorial Atlantic, between 7°N to 8° N, the Doldrums MTS displaces the MAR for about 630 km towards the east from 39.5°W to 34°W. Similar to other megatransforms, the Doldrums MTS defines a lens-shaped, 110 km-wide region of intense deformation. The average full spreading rate is approximately 30 mm/a (Cande et al., 1988), orthogonal to the MAR axis. Satellite-derived bathymetry and free-air gravity anomalies (Sandwell and Smith, 1997) suggest the occurrence of 3 ITRs bounded by 4 trans-

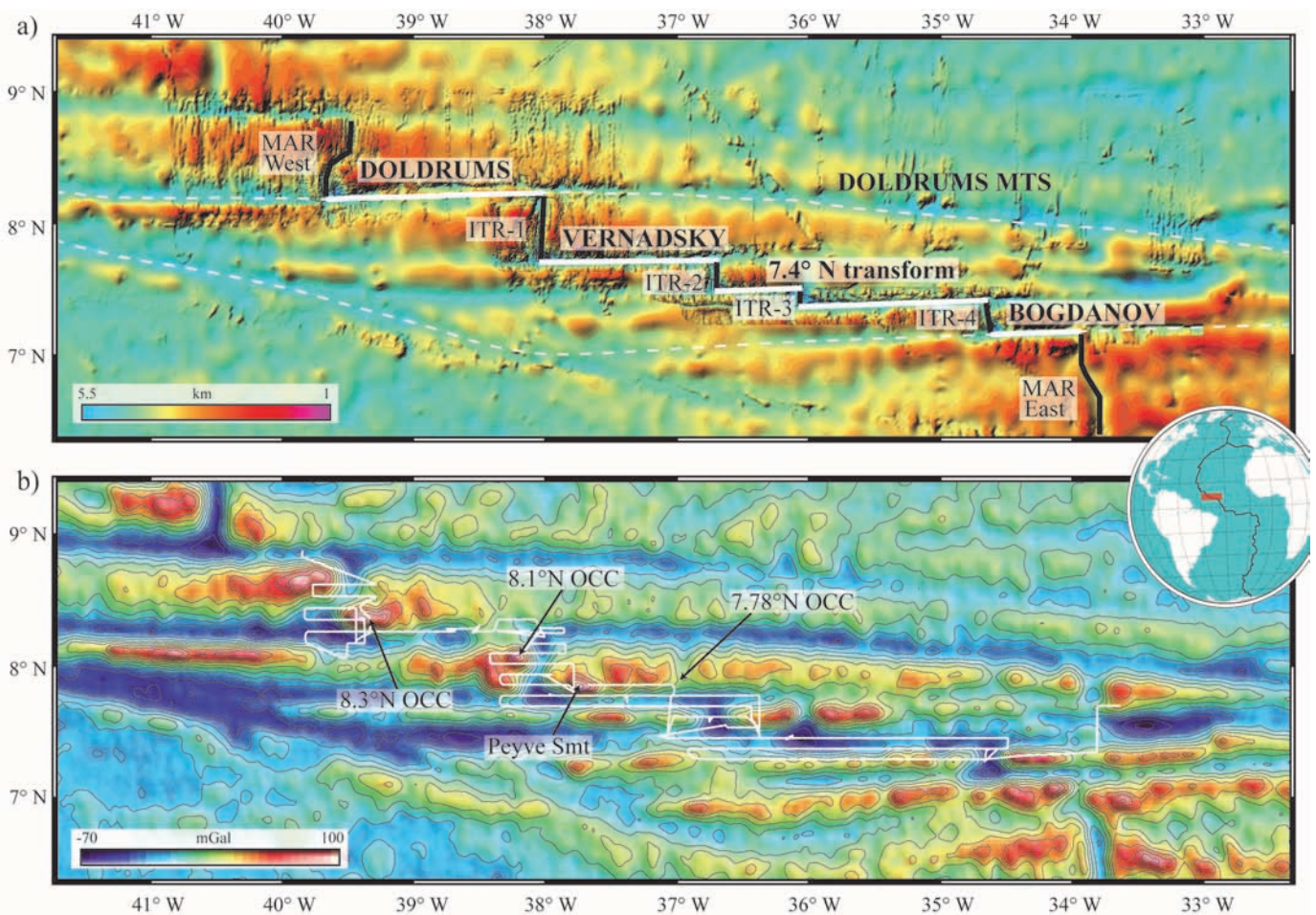


Fig. 1 - a) Doldrums MTS and associated intra-transform ridges and fracture zones offsetting the MAR superimposed upon the compilation of bathymetric data. b) Satellite-derived free air gravity field of the same area (Sandwell and Smith, 1997). Prominent structures described in the text are highlighted. Location of multibeam acquisition profiles is also indicated by white solid lines.

form valleys defined by the Doldrums, Vernadsky, 7.4°N and Bogdanov transforms (Fig. 1). However, on closer inspection, the 7.4°N transform may be divided in two strike-slip segments joined by a short ITR; this idea will be further confirmed by the bathymetric analyses of the present study. The length of transform offsets increases northward, reaching a maximum value of 177 km along the Doldrums transform. Considering a half spreading rate of 15 mm/a, the largest offset corresponds to an age offset of ~ 12 Ma. Previous multibeam surveys and dredge campaigns were conducted during cruises *R/V Strakhov* 6 and 9 (1987-88 and 1990) (Pushcharovsky et al., 1991; 1992). These cruises were mostly focused on the north-western portion of

the Doldrums MTS and along the northern sector of the MAR, between the Doldrums and the Arkhangelsky FZs. Twenty-seven and thirteen dredges, respectively, were deployed in several locations during expeditions 6 and 9 (hereafter S06 and S09). Dredging stations span from the MAR sector north of the Doldrums FZ, to the transform valley and to the south towards the ITR-1 (Fig. 1a). More dredges were also collected along the Vernadsky transform valley and on the shallowest part of its northern transverse ridge named Peyve seamount (Fig. 1b). Fig. 2a shows the location of dredge hauls from S06 and S09 expeditions, distinguished from those collected during our new expedition on the basis of the size of the pie charts.

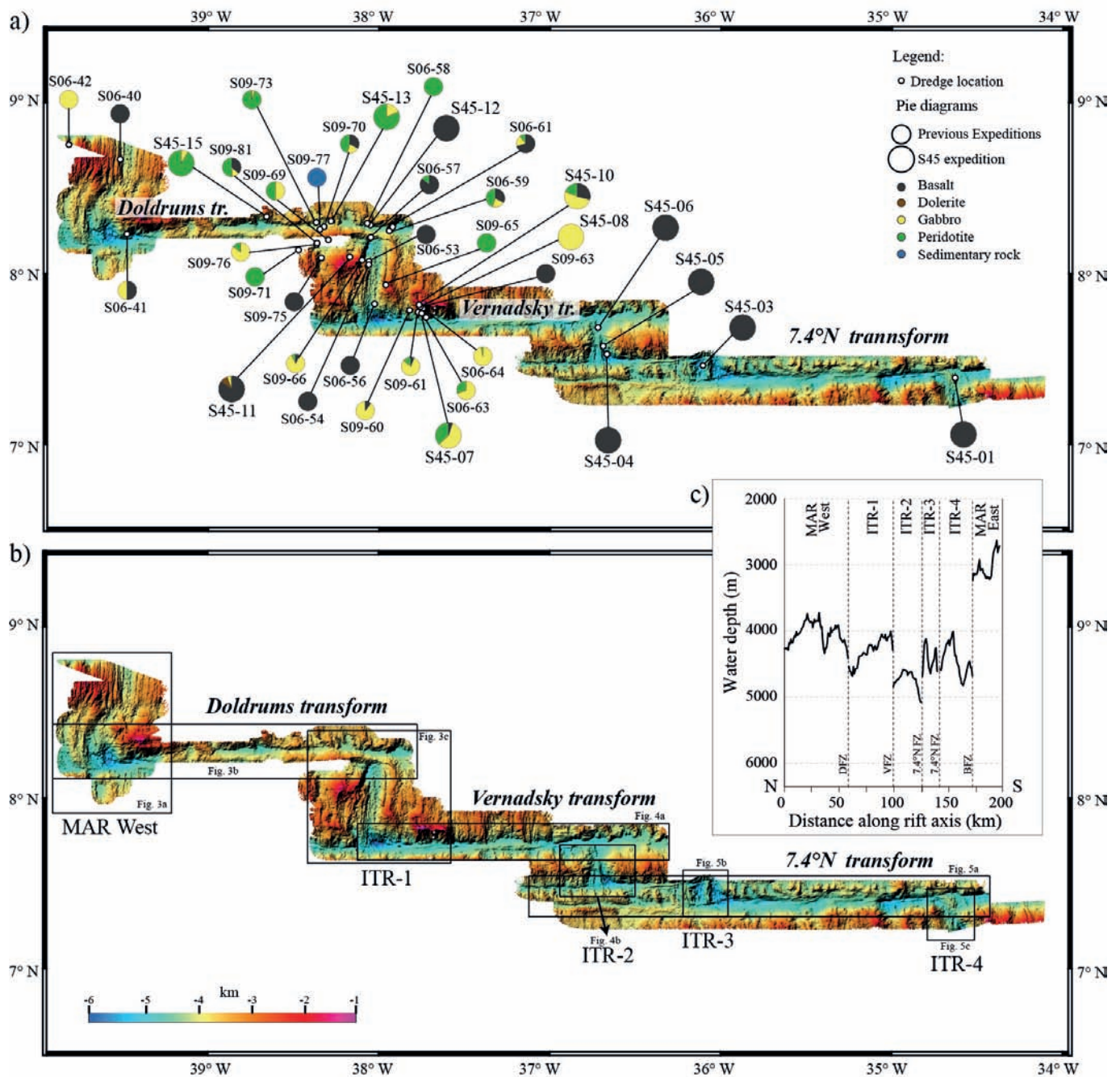


Fig. 2 - a) Shaded relief image of the Doldrums MTS obtained from swath bathymetry data acquired during the S45 expedition; grid resolution of 100 m; tr.- transform. Dredge locations from S06, S09 and S45 cruises are indicated by white dots. The pie diagrams refer to the compositional variability of lithologies (weight %) sampled in each dredge; large pie diagrams: S45 cruise; little pie diagrams: previous cruises. Locations of Figs. 3, 4 and 5 are indicated in (b). c) Axial depth profiles (direction N-S) along MAR-West, ITR-1, ITR-2, ITR-3, ITR-4 and MAR East; dotted vertical lines indicate the location of the transforms. DT- Doldrums transform; VT- Vernadsky transform; BT- Bogdanov transform.

The extensive dredging in the northern portion of the Doldrums MTS evidenced large regions of exposure of the oceanic basement along the Doldrums transform valley. This is typical of large fracture zone systems along the MAR, such as the 15°20'N (Kelemen et al., 2004), the Vema (Bonatti et al., 2005) and the Romanche FZs (Gasperini et al., 2001). One distinctive feature of the ITR-1 is, however, the occurrence of large portions of basement rocks including peridotites and deformed gabbros attributed to tectonic denudation through detachment faulting (Skolotnev et al., 2006). Here, rocks from the escarpment on the western wall of the rift valley, sampled during cruise 16 of *R/V Akademik Ioffe* in 2004, included fresh basalts and basalt breccia derived probably from the active axial volcanic ridge, along with gabbros ranging from highly deformed to severely altered. These hydrothermally altered rocks were considered as portions of the deepest zone of an active hydrothermal system located along a detachment surface.

#### 45th EXPEDITION OF *R/V AKADEMIC NIKOLAJ STRAKHOV*

The S45 expedition was carried out by the *R/V A.N. Strakhov*, which is equipped with differential GPS and SEAPATH positioning system. Bathymetry data were acquired using the 12 kHz RESON SEABAT-7150 71P multibeam system, consisting of 256 (2° x 2°) beams with a total aperture of 150° and capable to acquire data at full ocean depth. PDS-2000 by RESON was used to acquire and process the raw data to build 100 m and 50 m cell size grids, highlighting new evidence of the large-scale tectonic fabric of this poorly known area. A sound velocity probe hull-mounted 1 m above the Sonar Head and interfaced directly to the multibeam provides the real-time water velocity at transducers required for beam-forming. Sound velocity profile casts were taken twice per day to estimate the water column sound velocity and were integrated with the Levitus database. The multibeam data covered an area of about 29,000 km<sup>2</sup> and were collected along 18 E-W lines (total length is about 3,400 km) parallel to the five fracture zones forming the Doldrums MTS (Fig. 1). All the data presented in this work will be uploaded on a dedicated website or can be requested to the authors.

Seafloor sampling was achieved by using cylindrical dredges. Rocks collected were described on board, logged, sub-sampled and stored away; some rocks were cut and polished for thin section analyses. A total of 12 dredges out of 16 deployed in total recovered pillow basalts, dolerites, gabbroic rocks, peridotites, including tectonized varieties and sedimentary rocks. A detailed description of the dredge hauls is reported in the next sections and in Fig. 2a.

#### MORPHOLOGICAL CHARACTERISTICS OF THE DOLDRUMS MEGATRANSFORM SYSTEM

The morphological characteristics of the Doldrums MTS will be hereafter described from west to the east using the following terminology (see Fig. 2b). MAR West is the MAR segment approaching the Doldrums MTS from the north; ITR-1 represents the intratransform spreading centre between Doldrums and Vernadsky transforms; ITR-2 is located between Vernadsky and the northern valley of the 7.4°N transform; ITR-3 joins the northern and southern valleys of the 7.4°N transform; ITR-4 is located between the southern valley of the 7.4°N and the Bogdanov transforms. We also de-

finer other morphological features such as oceanic core complexes (OCCs) to indicate domed-shape structures related to exhumation of deep seated rocks by detachment faulting (after Cann et al., 1997).

#### MAR-West

The MAR segment approaching the Doldrums MTS consists of a 73 km-long rift valley subdivided by a nontransform offset into two ridge segments with different morphology (Fig. 3a). The northern segment displays a 30 km-long and 6 km-wide rift valley, with an average depth of ~ 4500 m. Its central part contains a narrow (500-800 m), 200 m-high neovolcanic ridge. Oceanic fabric typical of volcanic seafloor characterizes both sides of the rift valley, forming hills lined perpendicular to the spreading direction. The northern and southern ends of this segment display for a length of 8-10 km a series of small (1-2 km-wide) depressions reaching a depth of 4350 m alternated to isometric highs with an average depth of 3860 m. The rift valley of the southern segment is not obvious. Its central part reaches a depth of 3950 m and then abruptly deepens to 5600 m in the nodal basin at the Doldrums ridge-transform intersection (RTI).

The eastern side of the rift valley is characterized by a dome-shaped structure hereafter called 8.3°N OCC (Fig. 1b, 3a). This structure shows corrugations on the eastern flank defining a 30 x 35 km-wide corrugated surface. The summit reaches a depth of 1,300 m. The western side of the valley displays a prominent axial neovolcanic ridge parallel to the rift valley. This 6 km-wide volcanic ridge rises for 1,000 m above the base of the valley and extends to the south-east into the Doldrums transform (Fig. 3a).

#### Doldrums transform

The Doldrums transform consists of a right-lateral strike-slip fault with a length of 177 km and a width of 14-17 km. A ~ 130 km-long median ridge dissects the transform valley in its eastern sector. The median ridge is ~ 500 m high and is connected to the eastern shoulder of ITR-1. Rocks sampling during expedition S09 provided variably tectonized gabbros and predominantly peridotites (Fig. 3b, Pushcharovsky et al., 1991, 1992).

The northern wall of the Doldrums transform has a very rough topography. Its eastern sector consists of the southern terminations of abyssal hills penetrating into the transform valley with crests separated by depressions (4,500 m and 46,00 m), which likely represent old nodal basins. Dredges were deployed along the steep flanks of these structures at a distance of 185 (S45-12), 160 (S45-13) and 120 km (S45-15) from the MAR West axis. Most of these dredges recovered serpentinized and poorly deformed peridotites associated with minor Ox-bearing gabbros. Dredge S45-12 contained rounded rubbles of altered basalts with a thick Mn-coating, clearly derived from an ancient volcanic seafloor, and in agreement with the approximate age of ~ 12 Ma for the crust exposed in this sector of the fracture zone.

No bathymetric surveys were carried out along the valley to the south of median ridge in the current expedition, but its presence is confirmed by bathymetry data collected during previous cruises (S6).

#### Intratransform-1

The 55 km-long ITR-1 shows a symmetrical rift valley with a small (< 300 m high and 1 km wide) axial neovolcanic zone

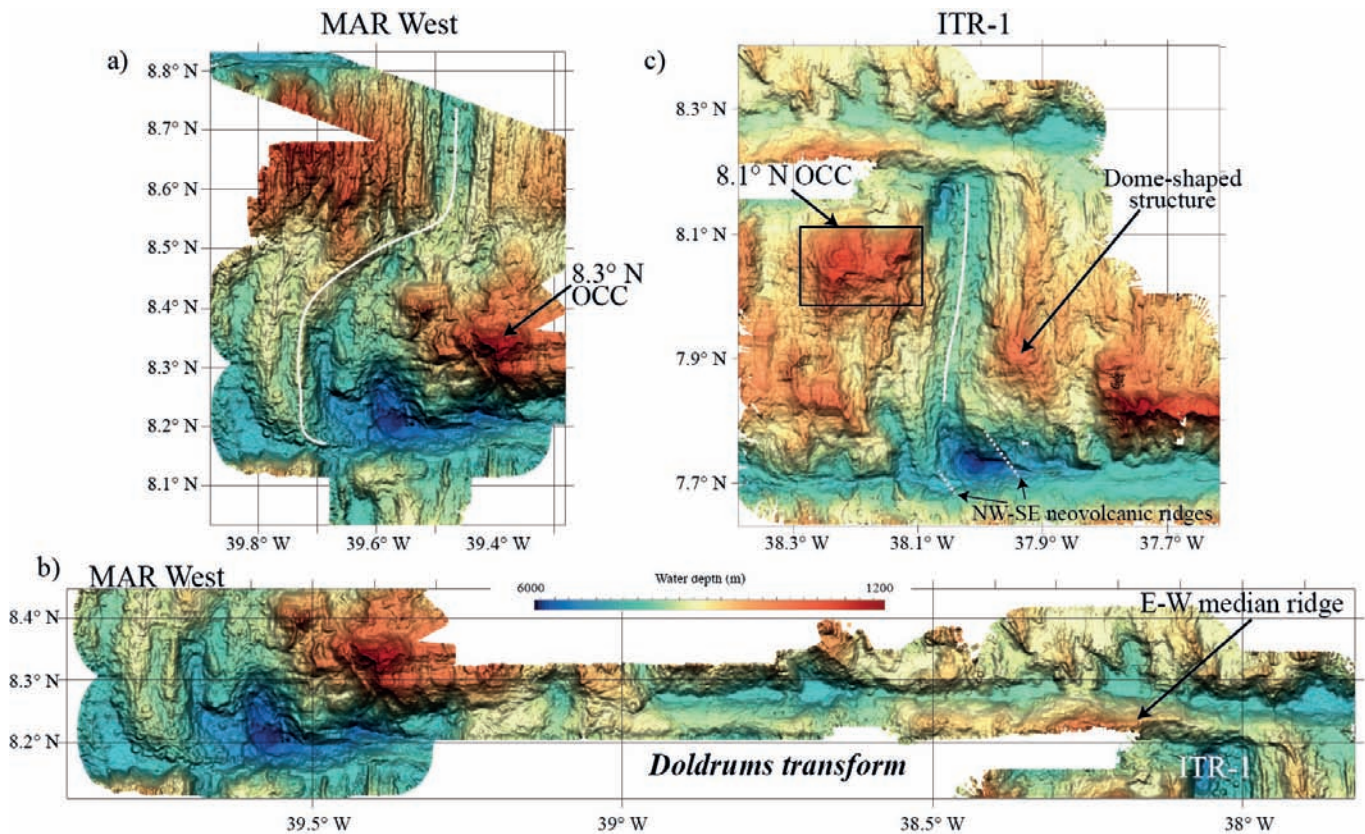


Fig. 3 - Details from the bathymetry of MAR-West (a); Doldrums transform (b) and ITR-1 (c). Structures described in the text are highlighted; white lines mark neovolcanic and axial ridges in MAR West and ITR-1, respectively.

elongated for the entire length of the ridge segment (Fig. 3c). To the north, the neovolcanic ridge is truncated by a well-developed median ridge that can be followed westwards along the Doldrums transform valley (see above). The volcanic activity appears mostly focused in the central portion of the rift valley. Here the axial valley is about 7 km-wide and 4,200-4,400 m-deep. Width and depth of the valley increase towards the south.

In the northern part of ITR-1, a dome-shaped structure, dominating the western flank of the rift valley, shows similarities with an oceanic core complex. The southern intersection with the Vernadsky transform has a large (7 × 15 km-wide) nodal basin, representing the deepest point of the entire Doldrums MTS (6,007 m). The nodal basin is flanked by prominent ridges up to 2 km wide and up to 400-600 m of relative height. The occurrence of fresh basalts dredged during S6 expedition (S06-56; Fig. 2) suggests a neovolcanic origin for these ridges. These ridges have NW-SE direction, different from the axial valley and from the N-S neovolcanic ridge in the northern part of the ridge segment. A small (diameter of 3-4 km) nodal basin, 5,100 m deep, is located at the northern RTI and on the western side of ITR-1. Dome-shaped morphologies are present also at the southern inner corner high that rises up to a depth of 2,450 m and evolves to the north into a ridge that is in continuity with the median ridge of the Doldrums transform.

#### 8.1°N Oceanic Core Complex

The dome-shaped structure located in the northern part of the ITR-1 in proximity of the Doldrums RTI, represents

an inner corner high (Fig. 3c). This structure is elongated perpendicular to the rift valley for 25 km, has a width of 18 km and rises from the bottom of the central rift for almost 3,000 m (Fig. 3c), with a summit approaching a depth of 1,600 m. The eastern flank of the OCC is characterized by a series of listric normal faults (~ 15°) plunging to the East, whereas to the south deepens towards a linear volcanic fabric. One dredge (S45-11) recovered abundant dolerites, gabbros, serpentinite schists and few fresh basalts. According to Skolotnev et al., (2006), the occurrence of cataclastic basalts and schistose peridotites may reveal the possible occurrence of a detachment fault, although bathymetry data recently collected do not show clear evidence of a corrugated surface.

#### Vernadsky transform

The Vernadsky transform offsets the MAR by ~ 145 km. The transform valley has a width of 10-12 km, and depths ranging from 4,700 to 4,900 m (Fig. 4a). E-W elongated highs interpreted as median ridges are stretched parallel to the transform valley. Their width reaches 3 km and a relative height of 500 m. The northern wall of the fracture zone has a complex structure, with two local structural highs that sharply stand out from the adjacent volcanic fabric of this area: (i) Peyve Seamount (Peyve Smt) and (ii) 7.78°N OCC. These structures will be described later. Similar to the northern wall of the Doldrums transform, abyssal hill terminations penetrate into the transform valley with crests separated by depressions, representing paleo nodal basins. Oceanic fabric on the southern wall of the Vernadsky fracture zone displays orientations varying from NW-SE to N-S. To the east, moving

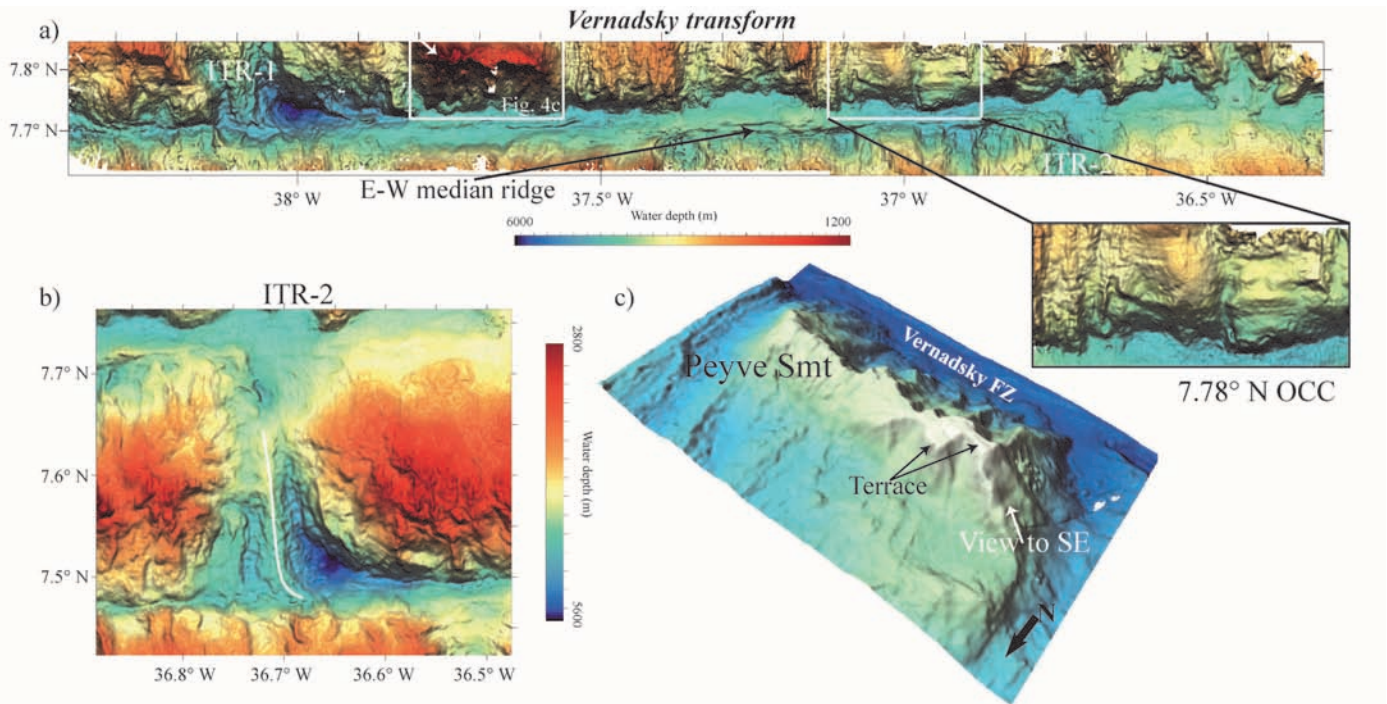


Fig. 4 - (a) Detailed bathymetry of the Vernadsky transform. The white boxes in the northern wall of the Vernadsky transform highlight the Peyve Smt and the 7.78°N OCC. (b) Detailed bathymetry of the ITR-2; the white line marks the axial ridge. (c) Three-dimensional view from NW of the Peyve Smt. Color scale from blue (deep) to white (shallow). Note the flat top constituted by two terraces.

towards the northern ITR-2 RTI, the seafloor is composed of unusual tectonic structures probably resulting from the interaction between processes leading to abyssal hills and OCCs formation. Two of these structures are shown in Fig. 4a.

#### Peyve Seamount (7.8 °N)

The Peyve Smt is a 37 km-long and 7 km-width structural high located 33 km to the east of the ITR-1 on the northern side of the Vernadsky transform (Fig. 4c). It is elongated parallel to the transform along the E-W direction with the western and eastern flanks shaped by high-angle normal faults plunging at  $\sim 25^\circ$ . The top of the seamount is flat and it is the shallowest point of the entire Doldrums MTS (993 m) rising up to 2,700 m above the transform valley floor. The Peyve Smt does not have any corrugated surface and according to its structural position and morphology may be regarded as a part of the northern transverse ridge of the Vernadsky transform. The flat summit may result from erosion at sea level.

Three dredges, deployed on the southern slope and at the top of the seamount, recovered prevalently gabbros and minor peridotites. The south slope is characterized by variably deformed gabbros (from porphyroclastic to ultramylonitic) ranging from moderately primitive (Ol-bearing) to highly evolved Ti-Fe oxide-gabbros. Cataclastic peridotites and gabbros were recovered at the top of the structure. Massive basalts were also collected at station S45-07 and more copiously at S45-10. Recovered lithologies recall those of the samples collected during expeditions S06 and S09 (Fig. 2a).

#### 7.78°N Oceanic Core Complex

Along the northern wall of the Vernadsky transform,  $\sim 130$  km to the east of ITR-1, an oceanic core complex exposes a  $\sim 20$  km-long and 8-km wide corrugated surface (Fig. 4a). Corrugations are elongated parallel to the transform valley

and are interrupted by deep scars as a result of subsequent high-angle normal faulting. The termination area deeps towards the west with an angle of  $\sim 6^\circ$  below a zone of linear hills oriented perpendicular to the spreading direction and regarded as the original volcanic hanging wall. The size and the structure of the corrugated surface recall those of the Kane megamullion nearby the Kane ridge-transform intersection at  $23^\circ 30'N$  along the MAR (Dick et al., 2008).

#### Intratransform-2

The ITR-2 is a 27 km-long symmetrical ridge segment with a robust volcanic activity. A huge neo-volcanic ridge ( $\sim 500$  m high and 15 km long) is located in the central and in the southern parts of the rift valley, near its western side, extending southward into the valley of the 7.4° N transform (Fig. 4b) where the ITR-2 displays a deep nodal basin (width of  $4 \times 10$  km) that reaches a depth of 5,720 m. Width and depth of the rift valley increase towards the south from 6 to 12 km and from 4,600 to 5,000 m, respectively. Western and eastern flanks (3,100-3,200 m) of the rift valley are uniform with no evidence of typical oceanic fabric or corrugated surfaces. Three dredges were deployed on the eastern rift shoulder where fresh basaltic glasses were recovered in the southern part (S45-04; S45-05), whereas partly altered basalts occurred in the northern sector (S45-06).

#### 7.4° N transform

The 7.4° N transform fault consists of two active dextral strike-slip zones joined by a very short intratransform spreading segment (ITR-3, Fig. 5a). The total length of the transform offset is 186 km. The northern transform valley is 5-6 km wide and 4,500-4,700 m deep, whereas the southern transform valley is 7-8 km wide and 4,500-4,900 m deep. The northern wall of 7.4°N transform, to the east of ITR-2, is characterized

by sigmoidal hills oriented NW-SE that turn WNW-ESE approaching the transform valley. Similar but more spectacular structures develop for nearly 60 km also to the east of ITR-3, where the seafloor is affected by several small sigmoidal hills (500-700 m-high) separated by parallel depressions oriented NW-SE that, close to the intersection with the transform valley, turn counter clockwise toward the WNW-ESE direction. Small sigmoidal ridges occur to the west of ITR-3 extending over a narrow band of  $\sim 20$  km. Straight ridges with similar strike are distributed further to the west of ITR-3.

The southern wall of the  $7.4^\circ\text{N}$  transform shows a distinct fabric. In particular, over a distance of  $\sim 25$  km to the west of ITR-4, we identify three abyssal hill crests striking N-S (500-700 m-height and 5-6 km-wide) separated by narrow parallel depressions. Further to the west there is a region of 70 km where isometric structures can be regarded as OCC. Two en-echelon E-W oriented transverse ridges run more further to west between  $36.25^\circ\text{W}$  and  $36.90^\circ\text{W}$ . The largest of these ridges is 2-3 km wide and about 42 km long, and has a relative height of 700 m. Further to the west there is a region of  $\sim 70$  km where isometric structures can be regarded as OCC (Fig. 5).

### Intratransform-3

ITR-3 is located in the deepest part of the Doldrums MTS. It is a short (16 km-long) intra-transform ridge segment with a prominent ( $\sim 1,200$  m-high) neovolcanic ridge extending for the entire length of the ITR and into the transform valleys (Fig. 5b). The rift valley is very wide reaching 17 km in width. Depths range from 5,000 to 5,400 m. The rift flanks are characterized by small sigmoidal structures that generally are not shallower than 4,000 m. These sigmoidal structures are oriented NW-SE and are most prominent in the SE section of the ridge axis. At both ends of axial region, two depressions with a complex morphology represent the nodal basins with a depth of 5,590-5,660 m. The axial neovolcanic ridge strikes N-S, orthogonal to the transforms. The overall sigmoidal shape of ITR-3 recalls geometries of a pull-apart basin. One dredge, deployed on the western flank of the axial valley, recovered fresh basalts and volcanic glasses.

### Intratransform-4

ITR-4 is 35 km-long and 15 km-wide spreading segment with bottom depth increasing southwards from 4,350 m to 5,050 m, and then abruptly decreasing towards the nodal basin (Fig. 5c). The axial valley is dominated by a  $\sim 1,000$  m-high and  $\sim 20$  km-long neovolcanic ridge located prevalently in the northern sector of the ridge segment. This neovolcanic ridge strikes along the NW-SE direction and extends northwards into the transform valley, where a nodal basin is absent. Dredging along the eastern flank of this volcanic ridge provided fresh pillow basalts with glass (S45-01). The rift valley is flanked to the east by a dome-shaped structure that reaches a water depth of 2,600 m and that most likely may represent an OCC. The western side of ITR-4 displays N-S oriented oceanic fabric. Finally, towards the south, the Bogdanov transform valley is dissected by an E-W elongated median ridge (previously mapped during expedition S22). This median ridge extends over the entire transform sector and intersects the prominent axial neovolcanic ridge of the MAR East.

## GEOPHYSICS

### Seismicity

In order to better define the present-day tectonic and magmatic activity over the entire Doldrums MTS, we carried out an analysis on seismicity based on instrumental recorded earthquakes occurred in the region. Earthquake parameters from January 1972 to December 2018 were obtained from the US Geological Survey Earthquake Catalogue (USGS). A total of 451 “reviewed” events with magnitude  $M_w > 3$  were gathered after converting different magnitudes types to momentum magnitude  $M_w$  adopting strategies and magnitude conversion formulas suggested by Lolli et al. (2014). Seismicity within the Doldrums MTS generally follows the typical distribution of slow spreading ridges with earthquake epicenters clustered along mid-ocean ridge segments and transform faults (Fig. 6). However, the seismicity distribution along the five transform faults and the four ITRs of the Doldrums MTS presents unusual peculiarities.

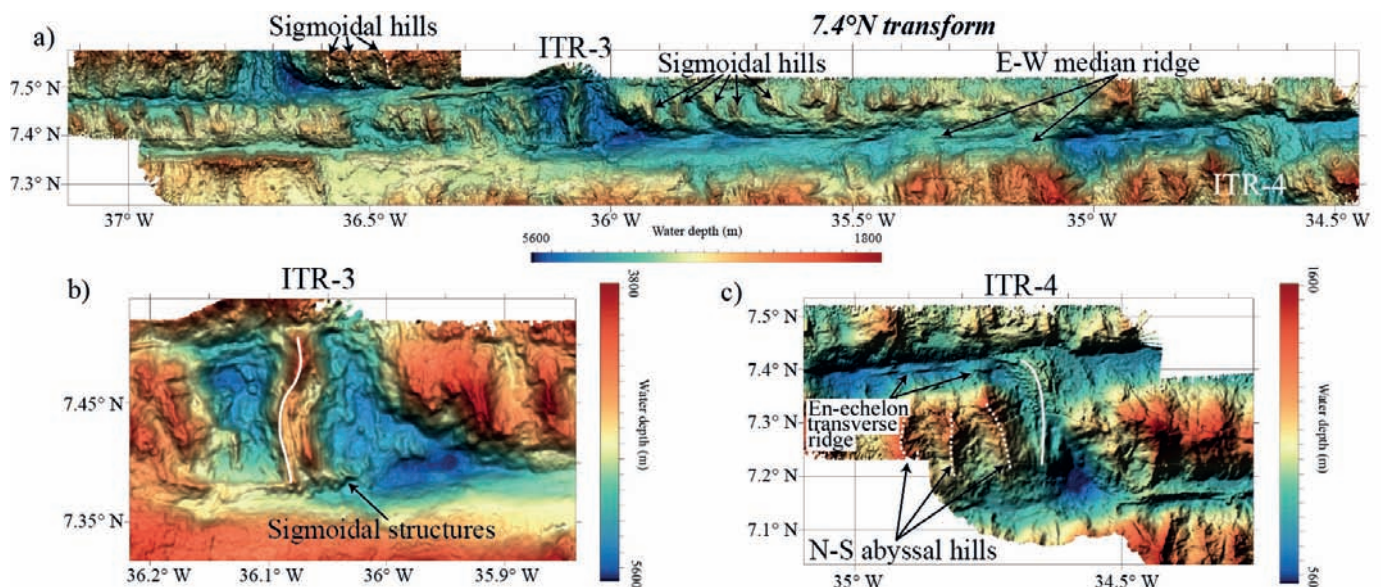


Fig. 5 - Detailed bathymetry of the  $7.4^\circ\text{N}$  transform (a) ITR-3 (b) and ITR-4 (c). Structures described in the text are highlighted; the white lines mark the axial ridges in ITR-3 and ITR-4.

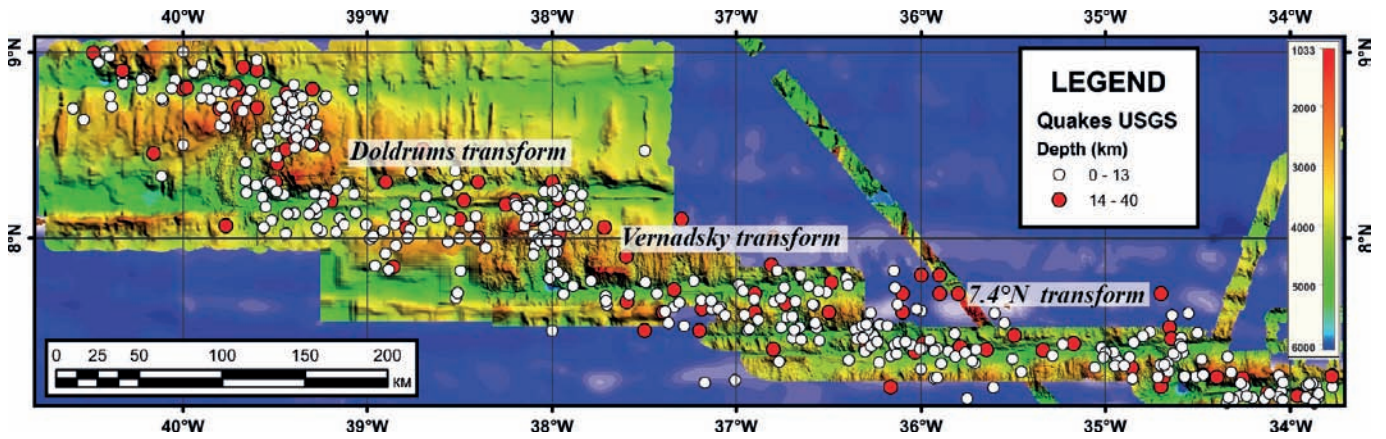


Fig. 6 - Seismicity of the Doldrums MTS region (from USGS earthquake catalogue) superimposed on multibeam bathymetry collected during S06, S09 and S45 expeditions of *R/V Akademik Nikolaj Strakhov* (1987-2019).

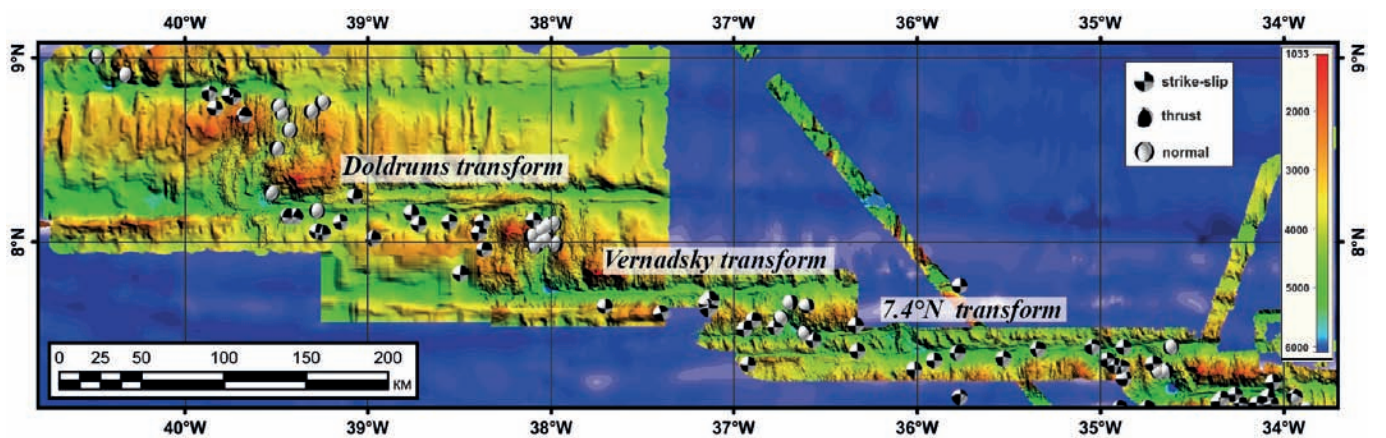


Fig. 7 - Harvard CMT focal mechanisms superimposed on multibeam bathymetry collected during S06, S09 and S45 expeditions of *R/V Akademik Nikolaj Strakhov* (1987-2019).

The USGS catalogue reports on only 10 events with magnitude  $M_w \geq 6$  to have occurred in this region, mostly distributed along the transform faults. Focal mechanisms from the global Centroid Moment Tensor (CMT) catalogue show right-lateral strike-slip movements on near vertical E-W striking fault planes (Fig. 7). Seismicity along transform faults depends on the offset length and slip rate and the maximum magnitude of earthquakes scales with it (Boetcherr and Jordan, 2004). Although the Doldrums MTS transforms have similar slip rates and offset lengths, most of these large events occurred along the southern valley of the Doldrums transform where the largest event in the region with a magnitude  $M_w$  of 7.0 took place on November 1<sup>st</sup>, 1984. This suggests that the present day Doldrums principal displacement zone is within the southern valley and that the Doldrums transform is seismically the most active strike-slip fault in the region.

Along the axial valleys and flanks of ITRs lower magnitude seismic events ( $M_w < 6$ ) occur with the exception of a large event with magnitude  $M_w = 6.1$  that took place on the eastern flank of the dome-shaped northern inner corner high of ITR-1 (8.1°N OCC). Fault plane solutions from the CMT database suggests normal faulting trending perpendicular to the seafloor spreading (Fig. 7). Seismicity distribution along the axis of ITRs shows a strong asymmetry with the large number of events clustered at the northern ridge-transform intersections. The observed poor seismicity at the southern

parts of intratransform spreading segments with the occurrence of corner highs and OCC along their eastern flanks, suggest that serpentinized upper mantle rocks may reduce the ability of stress accumulation, thus decreasing the number of detectable earthquakes.

### Gravity Bouguer anomalies

Bouguer gravity anomalies from the WGM2012 grid (Balmino et al., 2012) are shown in Fig. 8 together with the 3,000 m contour line in order to highlight the main bathymetric features of the region. The WGM2012 Bouguer grid includes gravity corrections aimed at remove the effect of the water layer using a crustal and water density of 2,670 and 1,027 kg/m<sup>3</sup>, respectively.

Negative Bouguer anomalies are centered along the major transform valleys, in particular, along the Arkhangelsky and the Vernadsky fracture zones suggesting relatively low-density rocks beneath transforms due to sedimentation and/or hydrothermal alteration of basement rocks including ultramafics serpentinization. Positive anomalies are centered mostly at inner corner highs, in particular at those where corrugated surfaces were observed suggesting exhumation of high-density deep-seated rocks at oceanic core complexes. However, gravity minima are also centered above some inner highs such as those located at the eastern RTI of the Arkhangelsky and

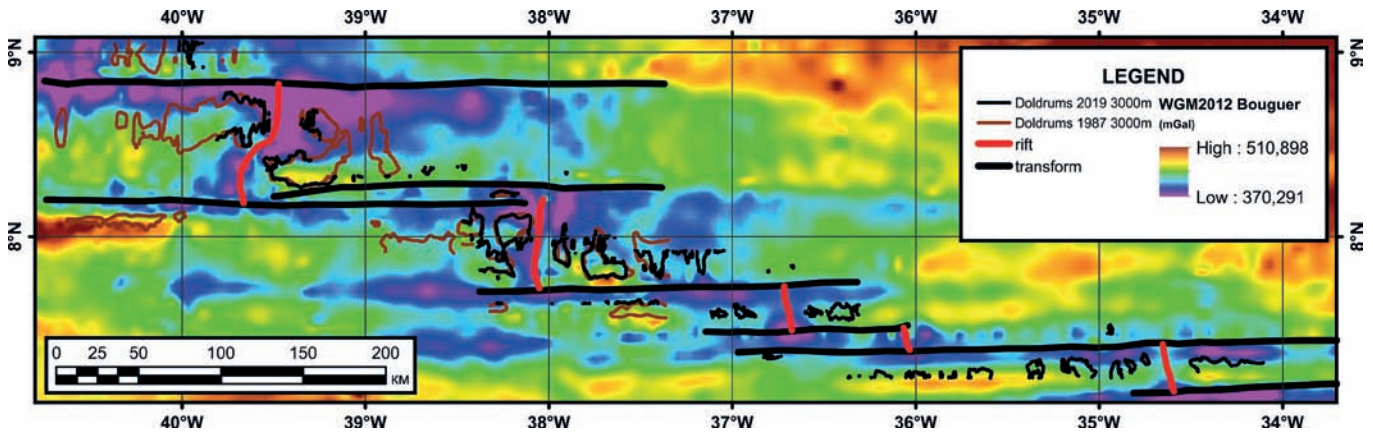


Fig. 8 - WGM2012 Bouguer anomalies and the 3000 m contour line (thick solid line) delineating the main structural features of the area.

the Doldrums transforms, probably related to a relative thick crust due to intense basaltic magmatism (Fig. 8). The western inactive part of the Doldrums fracture zone contains topography features similar to those observed in other transverse ridges such as that of Vema (Bonatti et al., 2003), although gravity anomalies are not very high on the southern flank of the transform valley.

**LITHOLOGIES**

During S45 we collected ~ 1,300 kg of rocks in 12 dredges deployed in different locations along the entire Doldrums MTS. Lithological proportions by weight are reported in Table 1 and in pie diagrams (Fig. 2a). Dredge hauls include basalt (~ 60 wt%), dolerite (~ 1 wt%), gabbro (~ 20 wt%) and peridotite (~ 19 wt%) (Fig. 9a). Few samples of sedimentary breccia and limestone were also recovered (< 0.5%). In the following sections we summarize rock descriptions divided per lithology.

We estimated mineral modal contents to define lithologies, and in basalts we defined vesicularity and phenocryst contents. Fresh glass and iron-manganese coating thicknesses were also measured. We used the semiquantitative scales from IODP Expedition 360 (MacLeod et al., 2017) to record the extent of alteration, and the crystal-plastic deformation and brittle intensities. Crystal-plastic deformation intensity was quantified based on the foliation, grain size, and relative proportions of neoblasts and graded from undeformed (grade 0) through clearly foliated (grade 2) to porphyroclastic (grade 3), mylonite and ultramylonite (grade 4 and 5, respectively). Brittle deformation was recorded from undeformed (grade 0), through fractured (grade 1), brecciated by numerous cracks without clast rotation (grade 2), densely fractured (grade 3), and well developed fault brecciation (grade 4) and cataclastic with grain size reduction > 70% (grade 5).

Fig. 9 - Lithology proportions and intensity of deformation for rocks recovered during the S45 cruise. a) Lithological proportion of S45 rocks (wt.%); from top to bottom we report the pie-chart diagrams of: all recovered samples, ultramafic rocks and gabbros, and all gabbros. The proportion of gabbros from the Peyve Smt is also shown separately. b) Semiquantitative evaluation of the crystal-plastic deformation intensity for S45 gabbros and peridotites based on ship-based observation.

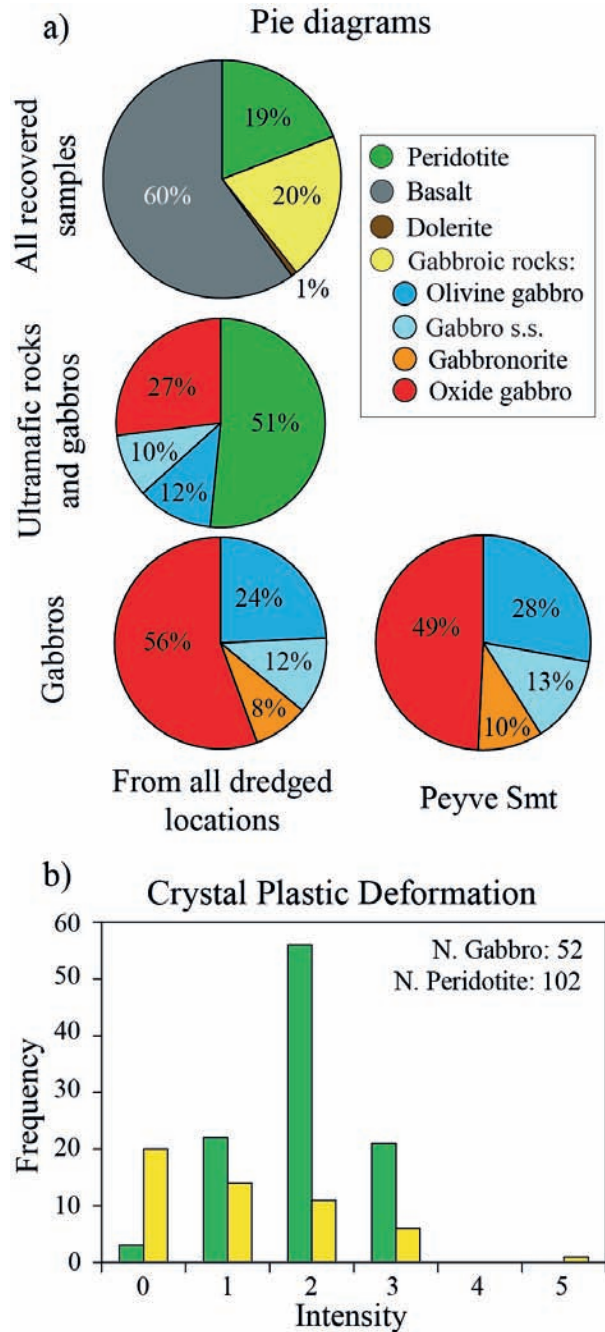


Table 1 - Location and general description of dredges deployed during the S45 expedition.

Dredge	Location of dredging	On Bottom			Off Bottom			Contents (%)							Weight (kg)
		Latitude (°N) (dd.ddd)	Longitude (°W) (dd.ddd)	Water depth (m)	Latitude (°N) (dd.ddd)	Longitude (°W) (dd.ddd)	Water depth (m)	Full (V) Empty (X)	Peridotite	Gabbro	Dolerite	Basalt	Breccia	Limestone	
S45-01	East flank of ITR-4	7.355	34.653	4430	7.357	34.652	4400	V				100			250
S45-02	East shoulder of ITR-4	7.287	34.623	4800	7.29	34.593	3700	X							
S45-03	West flank of ITR-3	7.463	36.107	5500	7.475	36.077	4160	V				100			50
S45-04	East shoulder of ITR-2	7.53	36.668	5600	7.535	36.653	4950	V				100			100
S45-05	East shoulder of ITR-2	7.577	36.69	5125	7.578	36.683	4990	V				100			35
S45-06	East shoulder of ITR-2	7.685	36.72	4960	7.683	36.717	4900	V				100			40
S45-07	South flank of Peyve	7.768	37.752	3800	7.76	37.773	3400	V	37	58		4	1		350
S45-08	Top of Peyve	7.807	37.76	1950	7.803	37.762	1900	V		100					5
S45-09	East flank of ITR-1	7.962	38	4250	7.987	37.992	3700	X							
S45-10	Top of Peyve SM	7.818	37.767	1100	7.822	37.762	1040	V	19	52		29			80
S45-11	North flank of 8°N OCC	8.098	38.172	3000	8.092	38.177	2570	V	1	5	9	85			250
S45-12	North wall of Doldrums FZ; 185 km from active ridge	8.285	38.052	4100	8.3	38.052	3600	V				98	2		10
S45-13	North wall of Doldrums FZ; 160 km from active ridge	8.308	38.282	3850	8.307	38.285	3770	V	81	18		1			100
S45-14	North wall of Doldrums FZ; 135 km from active ridge	8.287	38.503	3700	8.31	38.482	3230	X							
S45-15	North wall of Doldrums FZ; 120 km from active ridge	8.333	38.658	3160	8.335	38.657	3150	V	91	8			1		70
S45-16	North wall of Doldrums FZ; 35 km from active ridge	8.24	39.403	4600	8.247	39.402	4200	X							

### Basalt and dolerite

Based on preliminary evaluations dredged basalts were divided into three groups: (i) fresh, (ii) tectonized (mainly cataclastic) and (iii) basalts that went through substantial low temperature alteration.

Fresh basalt fragments are mainly angular and represent parts of pillow-lavas. Glass rims are fresh or slightly palagonitized and sometimes covered by thin Fe-Mn coating. Intact pillow basalts (Fig. 10a) and basaltic flows were recovered along the axial neovolcanic ridges of the intra-transform ridge segments, i.e. ITR-4 (dredge S45-01), ITR-3 (dredge S45-03) and ITR-2 (dredge S45-05 and S45-06). Fresh basalts were also collected on 8.1°N OCC (Dredge S45-11). Most basalts are aphyric to sparsely phyric (< 2% phenocrysts), and less than 20% are phyric (15-20% phenocrysts) with typically a microcrystalline matrix. Ol and plagioclase (pl) are present as phenocrysts in variable modal contents. Sparsely phyric basalts from dredge S45-11 are characterized by < 2% clinopyroxene (cpx) phenocrysts. Vesicularity is overall less than 5% by volume, with few samples showing up to 15% of vesicles. Fresh basalts display preserved glass from 2 to 20 mm in thickness.

The second group of basalts contains chlorite and generally displays evidence of incipient brittle deformation that locally develops to a cataclastic fabric with angular clasts of fractured basalts cemented by quartz (Fig. 11a). Tectonized basalts were collected at dredge S45-11 on the 8.1°N OCC.

Basalts with low temperature mineralizations contain smectites, Fe-hydroxides and thick Fe-Mn crust (up to 30 mm). Altered basalts were mainly found at the northern wall of the Doldrums transform valley in dredge S45-12. This dredge was deployed at ~ 180 km from the MAR-West axis and at an approximate age of ~ 12 Ma. Thus, due to a long exposure time at seafloor, these basalts have been significantly modified by seawater interaction.

Dolerites were exclusively recovered at dredge S45-11 on the 8.1°N OCC. These rocks are identified based on the occurrence of a visible crystalline matrix, presenting a sub-ophitic texture and locally including sporadic pl phenocrysts (Fig. 10b). All dolerite samples are altered as defined by the substitution of the original cpx by chlorite and pl by epidote and albite. Some samples are entirely replaced with hydrothermal minerals, also containing > 1 vol% of fine-grained disseminated pyrite (0.5-2.0 mm).

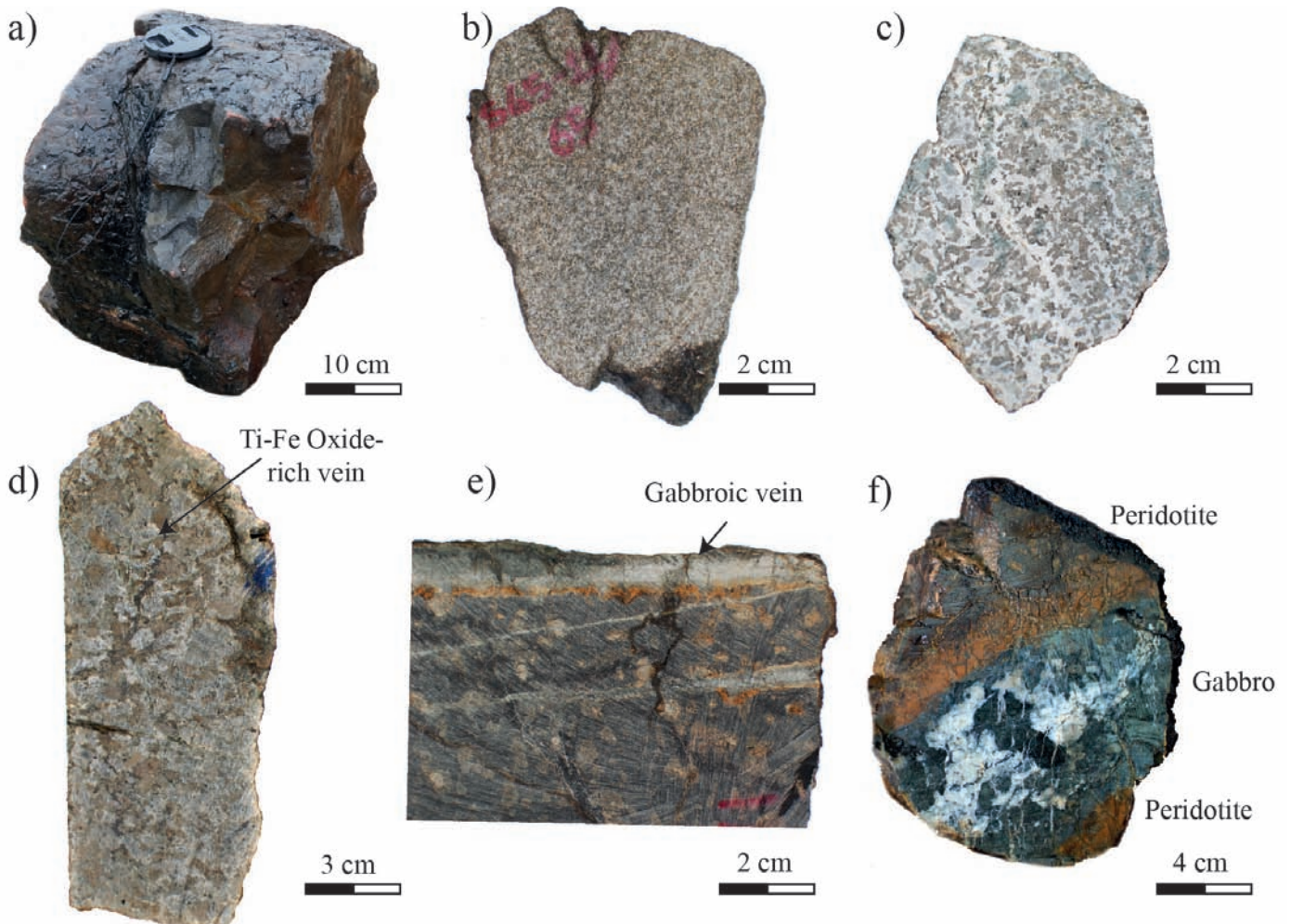


Fig. 10 - Photographs of S45 expedition samples showing the main lithologies. (a) sample S45-04/1 - fresh pillow lava from the east rift shoulder of the ITR-2. (b) sample S45-11/65 - medium-grained dolerite from the 8.1°N OCC. (c) sample S45-7/18 - medium-grained Ol-gabbro with sub-ophitic texture. (d) sample S45-15/15 - oxide-gabbro exhibiting Fe-Ti-Ox rich patches organized in microveins from the Peyve Smt. (e) sample S45-13/1 - coarse-grained partly serpentinized peridotite crosscut by two parallel gabbroic veins from the northern wall of the Doldrums transform. (f) sample S45-13/22 - peridotite crosscut by a oxide-gabbro vein (~7 cm). Note that the contact between the vein and the peridotites is marked by a pyroxene-rich layer (~2 cm-thick).

## Gabbro

Collected gabbros cover three principal varieties consisting of Olivine-gabbro (olivine, Ol > 5%), gabbro *sensu stricto* (Ol < 5%; Ti-Fe oxides, Ox < 2%), gabbroonorite (orthopyroxene [opx] > 5%) and Fe-Ti-Ox gabbro (Ox > 2%) (Fig. 9). They have a bimodal distribution, with nearly 25% of relatively primitive Ol-gabbro and > 50% of evolved oxides-gabbro. Ol-gabbros and gabbro *s.s.* have granular to subophitic textures, and are mostly medium-grained (Fig. 10c). Large cpx and, more rarely, Ol oikocrysts containing pl chadacrysts locally occur within the subophitic gabbro. Ol ranges from partly serpentinized showing the typical mesh texture, to largely preserved and altered by clay minerals. Opx in gabbroonorite has granular habit and is often replaced by a fine-grained assemblage of clay minerals. Fe-Ti oxides in oxide-gabbros occur as veins or discrete patches (Fig. 10d) locally forming cm-scale Ox-rich streams. Felsic veins are common within the samples, mostly limited to mm-scale

veins with sharp straight boundaries. In few cases felsic intrusions reach 2 cm in thickness and reveal the occurrence of interstitial amphibole and minor quartz. Fig. 11d shows a felsic vein intruding a slightly deformed Ol-gabbro. At the contact between the two rock-types, the Ol-gabbro is pervaded and partly disrupted by the felsic material and amphibole coronas develop around the pre-existing pyroxene, evidence of chemical interactions at high temperature. This reaction front can reach a thickness of 4 cm.

Most gabbros are tectonized to different extent. Deformation ranges from crystal plastic deformation (Fig. 9b) to low-temperature cataclasites (< 5%). Plastically deformed gabbros range from weakly deformed (Fig. 11b) to ultramytonitic (Fig. 11c). They are defined by mm-scale porphyroclastic pyroxene and pl mantled by neoblastic assemblages most likely made up of the same minerals. Amphibole veins are widely observed in deformed gabbros. These features suggest a high-temperature deformation event likely occurred under the granulite-facies conditions. One sample (S45-07/16) shows

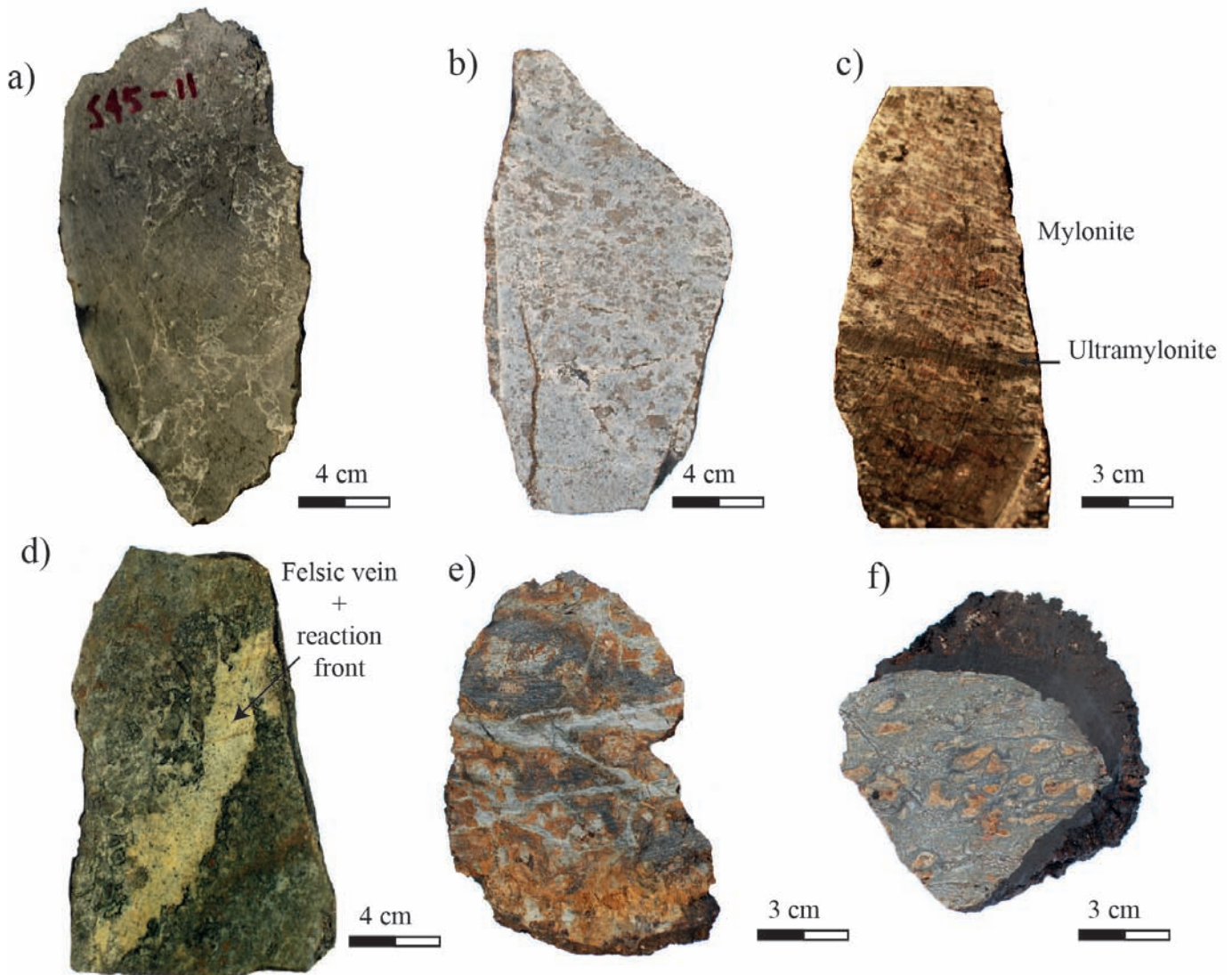


Fig. 11 - Photographs of variably tectonized S45 samples. (a) sample S45-11/82- basalt cataclasite cemented by quartz veins from the top of 8.1°N OCC (b) sample S45-07/22- coarse-to medium-grained gabbro weakly deformed under high temperature conditions. (c) sample S45-7/16- High temperature deformation gradient in gabbro showing a localization of the deformation from mylonitic to ultramytonitic band; Peyve Smt. (d) sample S45-10/2- deformed Ol-gabbro intruded by plagiogranite vein (~ 3cm) (Peyve Smt.). (e) sample S45-15/8- deformed peridotite with a dense network of fractures filled by basaltic material with microcrystalline texture. (f) sample S45-13/27- foliated peridotite mainly serpentine and covered by a thick Mn-coat from northern wall of the Doldrums transform.

a characteristic deformation gradient from porphyroclastic to mylonitic with a sharp contact with an ultramylonitic level (5 mm) (Fig. 11c), evidence for the localization of deformation at high temperature conditions. Deformed gabbros are mainly found in association with peridotites at the 8.1°N OCC (Dredge S45-11) and at the Peyve Smt (Dredges S45-07, 10). These rocks were also found in some dredges along the northern wall of the Doldrums transform (S45-13 and S45-15).

The most representative collection of gabbros was dredged on Peyve seamount. Fe-Ti oxide gabbro varieties (35%) in association with plagiogranite veins of different size and shape along with isotropic Ol- to Ol-free gabbro (5% and 17%, respectively) were found on this seamount. Such associations are typical of lower crust exposed at ridge-transform intersections along slow-spreading ridges (e.g., Dick et al., 2019), as well as at the dike-gabbro transition at fast spreading ridges such as the ODP Hole IODP 1256D (Pacific Ocean; Teagle et al., 2006).

### Peridotite

Harzburgites are the most common lithology among peridotites, but minor dunites are also present. Peridotite minerals are widely replaced by serpentine as effect of seawater interactions likely occurred at temperature < 500°C, and depths that close to the RTI can reach 15 km (Boschi et al., 2013). A minor amount of samples shows replacement of the original phases by clay minerals, classically attributed to superficial weathering. Collected peridotites record crystal plastic deformation with mainly porphyroclastic texture (Figs. 9b, 11f). Pyroxenite and gabbroic veins (ranging from gabbro to leucocratic in composition) are found in some peridotites. Gabbroic veins locally reach 10 cm in thickness and contain abundant Fe-Ti Ox (Fig. 11f). The occurrence of mafic veins indicates different events of melt migration and interaction with the lithospheric mantle. Peridotites are mainly found on the Peyve seamount, on 8.1°N OCC (Dredge S45-11, serpentine schists) and along the northern slope of Doldrums transform. These peridotites are always associated with gabbros, including deformed gabbros. Along the northern wall of the Doldrums transform we sampled peridotites at different distance eastward from the MAR west. Further studies will allow us to investigate mantle composition variations with time revealing differences in melt production.

### Sedimentary rocks

Few sedimentary rocks were collected at OCC 8.1°N (S45-11) and along the northern wall of the Doldrums transform (S45-15). They represent the tectono-sedimentary products of erosion and tectonic disruption of seafloor. Sedimentary rocks consist of polymictic breccia containing clasts of basalts, gabbros and serpentinized peridotites cemented by pelagic carbonates or by a silty matrix. Poorly sorted sandstones were also collected.

## DISCUSSION

### General architecture of the Doldrums megatransform system

The combination of data from previous expeditions S06 and S09 with those obtained during S45 allows us to present for the first time the large-scale structure of the Doldrums MTS. The bathymetric analysis confirms a complex

architecture with five dextral transform faults subdivided by four active ITRs. All the transform faults are characterized by median ridges with variable width and length, subdividing the transform valleys. Strike-slip earthquake epicenters concentrate along the transform faults and their distribution suggests southward migration of the principal displacement zone of the Doldrums transform (Figs. 6 and 7). The location of ITRs is confirmed by the occurrence of seismic clusters with normal focal mechanisms along the rift shoulders and by the occurrence of neovolcanic axial ridges. We are confident that the so-far unknown large-scale structure of the Doldrums MTS is now better defined.

One fundamental observation is that each ITR is characterized by different morphological features, suggesting a large variability in the tectonic conditions within this megatransform domain. The peripheral rift segments (i.e., ITR-1 and ITR-4) represent the shallower portions of the Doldrums MTS, whereas those located in the central part are substantially deeper (Fig. 2c). Considering that the axial depth of MOR is assumed to be dependent on the thermal conditions of the subridge mantle (Klein and Langmuir, 1987), this would imply a lower mantle temperature for the internal portion of the Doldrums MTS, or an overall transtensive regime in this megatransform system. We must note, however, that the neovolcanic ridges of ITR-2 and ITR-3 are characterized by large and high axial volcanic ridges, while ITR-1 and ITR-4 are characterized by large rift valleys and small axial volcanic ridges. The occurrence of prominent axial ridges formed by fresh pillow basalts is indicative of a strong magmatic production within ITR-2 and ITR-3. Indeed, the highest points of ITR-2 and ITR-3 locally reach the elevation of ITR-1 and ITR-4, as well as those of MAR segments outside the Doldrums region. In addition, the neovolcanic ridges of ITR-2 and ITR-4 prograde towards the south and north, respectively, into the adjacent transform valleys, in further agreement with a period strong magmatic production.

A sustained volcanic activity in the central ITRs contradicts expectations of reduced magmatism in short spreading centers due to the cold edge effect at ridge-transform intersections (e.g., Fox and Gallo, 1984; Bonatti et al., 1992). This is also at odd with numerical models that suggest that the innermost portions of a long-offset transform are characterized by a thick lithosphere (e.g., up to 45 km for a 900-km offset; Ligi et al., 2002). We must consider, however, that mantle composition plays a major role in the style and amount of mantle melting (e.g., Stracke and Bourdon, 2009); the more fertile is the mantle source, the highest melting degrees are expected. Hence, volcanism in the innermost portion of Doldrums MTS may have been triggered by the occurrence of an anomalous fertile component located in the asthenosphere, remobilized by the activation of a transtensive regime. Alternatively, the magmatic production in this region was highly discontinuous in time and the large volcanic ridges of ITR-2 and ITR-3 represent the expression of a recent period of strong magmatic activity. Although we prefer the first hypothesis, this idea needs to be tested with geochemical studies of the fresh basalt glasses collected in the ITRs.

In this framework, we can now speculate on the origin of ITR-3. The 7.4°N transform is subdivided in two active transform segments by a ~ 10 km-wide strongly-tectonized stripe of ocean floor. The latter is in turn crosscut by a lenticular depression representing the ITR-3 (Fig. 5a, b). According to dredge results, the huge neovolcanic zone within this ITR represents the youngest structure, and has N-S direction perpendicular to spreading direction. On the other

hand, the adjacent seafloor displays discordant sigmoidal hills that turn counter clockwise parallel to the transform valley. These structures recall extensional duplexes (Woodcock and Fischer, 1986) formed in an extensional dextral strike-slip system. Accordingly, we infer that the rift valley of ITR-3 may represent a pull-apart basin opened by a dextral strike-slip fault overstep (Fig. 5a, b). This idea is consistent with the occurrence of a prominent neovolcanic axial ridge, which testifies an abundant melt production and, by consequence, that the main lithospheric thinning was centered in this portion of the Doldrums MTS. The origin of this structure requires further analyses, and this model needs to be sustained by a throughout characterization of the volcanism in this region.

### Mechanisms of exposure of mantle and lower crustal rocks

In the previous sections we have shown that oceanic basement rocks are exposed in large regions at the Doldrums MTS. Basement exposures are typical of large fracture zones along the MAR, such as the 15° 20'N (Putscharovskiy et al., 1988; Kelemen et al., 2004), the Vema (Bonatti et al., 2005), Romanche (Ligi et al., 2002) and the St. Paul FZs (Hekinian et al., 2000). In this study we show four mechanisms responsible for the exhumation of deep-seated rocks on the seafloor.

(1) The most typical mechanism to expose basement rocks in a transform domain is the formation of transverse ridges (e.g., Bonatti et al., 2005). These features represent topographic anomalies oriented parallel to the transform valley and exposing continuous sections of oceanic lithosphere (e.g., Auzende et al., 1989). Geophysical and sampling investigations suggest that these slabs of oceanic lithosphere are uplifted during changes in transform-related tectonics (Kastens et al., 1998). A similar origin is suggested here for the transverse ridges exposed along the fracture zones of our study area. One possible example is the Peyve Smt (Fig. 4c). This structure forms the northern wall of the Vernadsky transform, elongated for ~ 30 km parallel to the transform valley. In many aspects it is similar to known transverse ridges formed on the northern side of the Romanche FZ (Ligi et al., 2002) and on the southern side of the Vema FZ (Bonatti et al., 2005), but differs by smaller dimensions. According to the dredging results of S09 and S45, this structure exposes a section made up by peridotites and gabbros. The top of the sequence is most likely formed by deformed gabbros, which show a continuum from granulite-facies conditions (> 800°C) to low temperature brittle cataclastic deformation. We note that the gabbros exposed on the Peyve Smt are mainly evolved oxide-gabbros, whereas primitive terms are lacking (Fig. 9). This may be due to a sample bias or, more likely, may indicate that the oceanic lower crust is mostly constituted by evolved terms. The same characteristics were documented by Brunelli (personal communication) in the transverse ridge of the Vema FZ, and interpreted as a consequence of extreme fractionation and longitudinal flow of magma from the segment center towards the transform. The widespread exposure of oxide-gabbros is also characteristic of the intersection between the Atlantis Bank OCC and the Atlantis II transform wall, in the SWIR, where Dick et al. (2019) reported an overall higher amount of evolved lithologies compared to Holes 735B and 1473A, in turn located in the medial portion of the same OCC (see Dick et al., 2000; MacLeod et al., 2017). The flat top of the Peyve Smt (Fig. 4c)

and the lack of a basaltic layer suggest that this seamount was eroded in a subareal or shallow marine environments. Further analyses are necessary to understand the origin of this seamount, however it lacks corrugations and its location along the transform valley lead us to speculate that this transverse ridge formed under transpressive conditions in contrast with a transtensive origin for the Vema transverse ridge. Longer, but smaller transverse ridges were also detected on the southern flank of the 7.4° transform, but not easily interpreted due to the lack of a complete survey.

(2) Another mechanism able to expose basement rocks is the formation of median ridges. These features were firstly recognized in the Romanche FZ by Bonatti et al. (1974) and later in the Vema FZ and in the Indian and Pacific oceans (e.g., Lagabriele et al., 1990; Dick et al., 1991; Gallo et al., 1986). Initially, they were interpreted as resulting from the diapiric rise of serpentinized mantle peridotites within the transform valley (Macdonald et al., 1986; Dick et al., 1991). Another interpretation seems to indicate that these are portions of the oceanic mantle uplifted by isostatic rebound (Detrick et al., 1982) or tectonic extension during the formation of a nodal basin (Lagabriele et al., 1992). Median ridges are found in all the transforms of the Doldrums MTS (Fig. 2b). They bisect the transform valleys in two transform segments, but show a great variability in size and morphology. The largest median ridge is exposed within the Doldrums transform, covering most of the active transform valley (Fig. 3b). Dredging during S09 reveals the occurrence of peridotites and minor deformed oxide-gabbros, similar to those collected in the transverse ridges (Fig. 2a). Since these rocks are relatively un-serpentinized, an origin by diapiric rise seems unlikely. The continuity of most of these median ridges with abyssal hills along the ITRs leads us to prefer an origin through tectonic extension following the formation of nodal basins.

(3) The shallowest portions of the rift shoulders are represented by the summits of oceanic core complexes. They consist in dome-shaped bodies exhumed through detachment faulting. First recognized at 30°N in the MAR (Cann et al., 1997), OCC have been mapped in several locations along the MAR and are now considered a fundamental style of seafloor spreading at slow and ultra-slow spreading ridges (e.g., Escartin et al., 2008; 2017; Smith et al., 2014), as well as in back-arc basins (Ohara et al., 2001). One fundamental feature of OCCs is the occurrence of corrugations representing the exposure of the detachment fault surface. In our study area, we found several OCCs located along the transform walls or in the inner corner highs. OCCs are commonly formed in association with nodal basins. Amongst the OCCs exposed in the area, the 8.1°N OCC was extensively dredged (Fig. 3c). It consists of highly tectonized gabbros and chloritized basalts. The occurrence of serpentine schists with sliding surfaces led us to suggest an exhumation process through detachment faulting (Fig. 11). The textural features of the gabbros are consistent with this interpretation, revealing a retrograde tectono-metamorphic evolution typical of OCCs worldwide (e.g., Dick et al., 2000; Boschi et al., 2006; Blackmann et al., 2006; MacLeod et al., 2017; Sanfilippo et al., 2018). For instance, these rocks retain textural evidence for high temperature deformation developed at hyper-solidus conditions, followed by the formation of amphibole-rich veins and, finally, by low-grade metamorphism (Skolotnev et al., 2006). Another interesting OCC has been detected at 7.78°N and 36.96°W along the 7.4°N transform (Fig. 4a). At a distance of 130 km from the ITR-1, we can infer an age of

approximately 8.5 Ma. The detachment surface has large-scale well-developed corrugations covering an area of 160 km<sup>2</sup> cut in its central sector by two conjugated normal faults. Although we could not deploy any dredge along this OCC during S45, we stress that this represents an optimum location to collect lower crustal and mantle lithologies formed in the early stage of evolution of the Doldrums MTS. The striking similarity with the well-known Kane Megamullion core complex at 23°N along the MAR (see Dick et al., 2008) makes the 7.4°N OCC an ideal location to substantiate our knowledge on detachment faulting as an important accretionary process at slow spreading ridges.

(4) A last fundamental location where mantle peridotites and gabbros were collected in the Doldrums MTS are the cliffs of abyssal hills facing the transform valleys. These structures often constitute the walls of the transform valleys where neither detachment faults nor transverse ridges are observed. The best examples are exposed at the northern wall of the Doldrums transform (Fig. 3b), where dredges S45-13 and S45-15 collected peridotites and gabbros (Fig. 2a). We speculate that these cliffs represent the southward continuation of abyssal hills into the transform valley and delineate high-angle normal faults resulting from the opening of the axial valley. In contrast to the formation of a heterogeneous oceanic lithosphere exposed by detachment faulting, high-angle normal faults at slow spreading ridge are typically related to the development of a “normal” oceanic lithosphere, or in the hanging wall of asymmetric rift system (see Wernicke, 1985; Lagabriele et al., 1990). This idea is sustained by geochemical investigation of the magmatism developed during detachment faulting which, in line with numerical and thermodynamic modelling, suggests that the magma budget plays a major role in the style of accretion of the oceanic lithosphere at slow spreading ridges (e.g., Escartin et al., 2008; Tucholke et al., 2008; Smith et al., 2014; Sanfilippo et al., 2018). Accordingly, the exposure of basement rocks along these high-angle normal faults allows investigating the accretionary process of what can be regarded as the “normal” volcanic seafloor formed in period of sustained magmatic activity. Preliminary results from geochemistry of the peridotites dredged during S06 and S09 expeditions show highly depleted compositions and a residual character (Sanfilippo, person. comm.), further supporting the idea of high degree of mantle melting and high magma budget in the Doldrums region.

## CONCLUSIONS

The enormous amount of the new data collected during cruise S45 allow us to define for the first time the large-scale structure of the Doldrums MTS. Coupled with data from previous expeditions we can now anticipate some fundamental inferences on the formation and evolution of this unknown megatransform domain. The main conclusions of this study are summarized below:

1. Four seismically active intra-transform spreading segments subdivide the Doldrums MTS into five transform segments, which are well delineated by seismicity distribution and dextral strike-slip seismic fault plane solutions.
2. Although the axial depth of ridge segments decreases from the peripheral portions of the megatransform towards the innermost sectors, the central ITRs contain large neovolcanic axial ridges locally protruding within the transform valleys. This is indicative of abundant magmatic activity

and may suggest a zone of high degree of mantle melting and/or active mantle upwelling in the central part of the Doldrums MTS. We speculate that this may be a consequence of a transtensive regime possibly centered in a zone of anomalous fertile asthenosphere.

3. Structural highs and dome-shaped structures are mostly represented by oceanic core complexes (i.e., 8.3°N OCC; 8.1°N OCC; 7.78°N OCC). Dredging results on some of these features provided deformed mantle and lower crustal rocks typical of OCC worldwide agreeing with exhumation through detachment faulting. This view is also supported by positive Bouguer gravity anomalies centered on these structures suggesting emplacement of rocks with higher density. Deformed gabbros and positive Bouguer gravity anomaly also characterize the Peyve Smt., which is in turn interpreted as a portion of transverse ridge uplifted during a transpressive regime.
4. Large regions of basement exposure characterize the transform valleys and the ridge transform intersections. Four different mechanisms may be responsible for the exposure of basement rocks. They are: (i) formation of transverse ridges along the transform valleys (i.e., Peyve Smt); (ii) uplift of median ridges within the transform valleys; (iii) denudation of basement rocks and formation of the OCCs by detachment faulting at inner corner highs and (iv) exposure of deep-seated rocks at the footwall of high-angle normal faults at the ridge-transform intersections.

## ACKNOWLEDGMENTS

We would like to thank the captain, the officers and the crew of *R/V Akademik Nikolaj Strakhov*. The chief scientist Elena Ivanova is also kindly thanked. This study was supported by the Russian Foundation for the Basic Research (project no. 18-55-7806 Ital\_t, 18-05-00001, 18-05-00691), Russian Basic Research Program (projects no. 0135-2019-0050, 0135-2019-0076, 0137-2019-0012, 0136-2018-0025), by Accordo Bilaterale CNR/RFBR 2018-2020 (CUP-B36C17000250005) and by the Italian Programma di Rilevante Interesse Nazionale (PRIN\_2017KY5ZX8). The study benefited of constructive reviews by P. Tartarotti and one anonymous reviewer.

## REFERENCES

- Auzende J.M., Bideau D., Bonatti E. et al., 1989. Direct observation of a section through slow-spreading oceanic crust. *Nature*, 337: 726-729.
- Balmino G., Vales N., Bonvalot S. and Briais A., 2012. Spherical harmonic modeling to ultra-high degree of Bouguer and isostatic anomalies. *J. Geod.*, 86: 499-520.
- Blackman D. K., Ildefonse B., John B.E. et al. 2006. Oceanic core complex formation, Atlantis massif, Proceed. Integr. ODP, 304/305: 304-605, <https://doi.org/10.2204/iodp.proc.304305.2006>.
- Boettcher M.S. and Jordan T.H., 2004. Earthquake scaling relations for mid-ocean ridge transform faults. *J. Geophys. Res.*, 109: B12302.
- Bonatti E., 1978. Vertical tectonism in oceanic fracture zones. *Earth Planet. Sci. Lett.*, 37 (3): 369-379.
- Bonatti E., Brunelli D., Buck W.R. et al., 2005. Flexural uplift of a lithospheric slab near the Vema transform (Central Atlantic): Timing and mechanism. *Earth Planet. Sci. Lett.*, 240: 642-655.
- Bonatti E., Brunelli D., Fabretti P. et al., 2001. Steady-state creation of crust-free lithosphere at cold spots in mid-ocean ridges. *Geology*, 29: 979-982.

- Bonatti E., Emiliani C., Ferrara G. et al., 1974. Ultramafic-carbonate breccias from the equatorial Mid Atlantic Ridge. *Mar. Geol.*, 16 (2): 83-102.
- Bonatti E., Ligi M., Borsetti M. et al., 1996a. Lower Cretaceous deposits trapped near the equatorial Mid-Atlantic Ridge. *Nature*, 380, 518-520.
- Bonatti E., Ligi M., Brunelli D. et al., 2003. Mantle thermal pulses below the Mid-Atlantic Ridge and temporal variations in the formation of oceanic lithosphere. *Nature*, 423: 499-505.
- Bonatti E., Ligi M., Carrara G. et al., 1996b. Diffuse impact of the Mid Atlantic Ridge with the Romanche transform: an Ultracold Ridge/Transform Intersection. *J. Geophys. Res.*, 101: 8043-8054.
- Bonatti E., Peyve A., Kepezhinskas N. et al., 1992. Upper mantle heterogeneity below the Mid-Atlantic Ridge, 0°-15°N. *J. Geophys. Res.*, 97, B4: 4461-4476.
- Boschi C., Bonatti E., Ligi M. et al., 2013. Serpentinization of mantle peridotites along an uplifted lithospheric section, Mid Atlantic Ridge at 11°N. *Lithos*, 178: 3-23.
- Boschi C., Früh-Green G.L. and Escartín J., 2006. Occurrence and significance of serpentine-hosted, talc- and amphibole-rich fault rocks in modern oceanic settings and ophiolite complexes: An overview. *Ophioliti*, 31 (2): 129-140.
- Cande S.C., LaBrecque J.L. and Haxby W.F., 1988. Plate kinematics of the south Atlantic, chron C34 to the present. *J. Geophys. Res.*, 93: 13479-13492.
- Cann J.R., Blackman D.K., Smith D.K. et al., 1997. Corrugated slip surfaces formed at ridge-transform intersections on the Mid-Atlantic Ridge. *Nature*, 385 (6614): 329-332, <http://dx.doi.org/10.1038/385329a0>.
- Cannat M., Sauter D., Mendel V. et al., 2006. Modes of seafloor generation at a melt-poor ultraslow-spreading ridge. *Geology*, 3 (7): 605-608, <https://doi.org/10.1130/G22486.1>.
- Detrick R.S., Cormier M.H., Prince R.A. et al., 1982. Seismic constraints on the crustal structure within the Vema Fracture Zone. *J. Geophys. Res.*, 87: B13, <https://doi.org/10.1029/JB087iB13p10599>.
- Dick H.J.B., MacLeod C.J., Blum P. et al., 2019. Dynamic accretion beneath a slow-spreading ridge segment: IODP Hole 1473A and the Atlantis Bank Oceanic Core Complex. *J. Geophys. Res.*, Solid Earth. *Am. Geophys. Union*, [ff10.1029/2018JB016858f](https://doi.org/10.1029/2018JB016858f).
- Dick H.J.B., Natland J.H., Alt J.C. et al., 2000. A long in situ section of the lower ocean crust: results of ODP Leg 176 drilling at the Southwest Indian Ridge. *Earth Planet. Sci. Lett.*, 179 (1): 31-51.
- Dick H.J.B., Schouten H., Meyer P.S. et al., 1991. Tectonic evolution of the Atlantis II fracture zone. In R.P. Von Herzen, P.T. Robinson et al. (Eds.), *Proceed. ODP Sci. Res.*, 118: 359-398, <http://dx.doi.org/10.2973/odp.proc.sr.118.156.1991>.
- Dick H.J.B., Tivey M.A. and Tucholke B.E., 2008. Plutonic foundation of a slow-spreading ridge segment: oceanic core complex at Kane Megamullion, 23°30'-N, 45°20'-W. *Geochem. Geophys. Geosyst.*, 9 (5): Q0501, <http://dx.doi.org/10.1029/2007GC001645>.
- Escartín J., Mevel C., Petersen S. et al., 2017. Tectonic structure, evolution, and the nature of oceanic core complexes and their detachment fault zones (13°20'-N and 13°30'-N, Mid Atlantic Ridge). *Geochem. Geophys. Geosyst.*, 18 (4): 1451-1482.
- Escartín J., Smith D.K., Cann J. et al., 2008. Central role of detachment faults in accretion of slow-spread oceanic lithosphere. *Nature*, 455 (7214): 790-794.
- Fox P.J. and Gallo D.G., 1984. A tectonic model for ridgetransform-ridge plate boundaries: Implications for the structure of oceanic lithosphere. *Tectonophysics*, 104 (3-4): 205-242.
- Gallo D.G., Fox P.J., Macdonald K.C., 1986. A Sea Beam investigation of the Clipperton Transform Fault: the morphotectonic expression of a fast slipping transform boundary. *J. Geophys. Res.*, 91 (B3): 3455-3467.
- Gasparini L., Bernoulli D., Bonatti E. et al., 2001. Lower Cretaceous to Eocene sedimentary transverse ridge at the Romanche Fracture and the opening of the of the equatorial Atlantic. *Mar. Geol.*, 176 (1-4): 101-119.
- Hekinian R., Juteau T., Gràcia E. et al. 2000. Submersible observations of Equatorial Atlantic mantle: The St. Paul Fracture Zone region. *Mar. Geophys. Res.*, 21: 529, <https://doi.org/10.1023/A:1004819701870>.
- Kastens K., Bonatti E., Caress D., Carrara G., Dauteuil O., Früh-Green G., Ligi M. and Tartarotti P., 1998. The Vema transverse ridge (Central Atlantic). *Mar. Geophys. Res.*, 20: 533.
- Kelemen P.B., Kikawa E., Miller D.J. et al., 2004. ODP Leg 209 drills into mantle peridotite along the Mid-Atlantic Ridge from 14°N to 16°N. *JOIDES J. Proceed. ODP 209 Initial Rep.*, 30 (1): 14-19.
- Klein E.M. and Langmuir C.H., 1987. Global correlations of ocean ridge basalt chemistry with axial depth and crustal thickness. *J. Geophys. Res.*, 92: 8089-8115.
- Lagabrielle Y. and Cannat M., 1990. Alpine Jurassic ophiolites resemble the modern central Atlantic basement. *Geology*, 18: 319-322.
- Lagabrielle Y., Mamaloukas-Frangoulis V., Cannat M. et al., 1992. Vema Fracture Zone (Central Atlantic): Tectonic and magmatic evolution of the median ridge and the eastern ridge-transform intersection domain. *J. Geophys. Res. Solid Earth*, 97 (B12): 17331-17351.
- Ligi M., Bonatti E., Cipriani A. and Ottolini L., 2005. Water-rich basalts at mid-ocean-ridge cold spots. *Nature*, 434: 66-69.
- Ligi M., Bonatti E., Gasparini L. and Poliakov A.N.B., 2002. Oceanic broad multifault transform plate boundaries. *Geology*, 30: 11-14.
- Lolli B., Gasparini P. and Vannucci G., 2014. Empirical conversion between teleseismic magnitudes ( $M_b$  and  $M_s$ ) and moment magnitude ( $M_w$ ) at the Global, Euro-Mediterranean and Italian scale. *Geophys. J. Int.*, 199: 805-828.
- MacLeod C.J., Dick H.J.B., Blum P. et al., 2017. Expedition 360 summary. In: C.J. MacLeod, H.J.B. Dick., P. Blum and the Expedition 360 Scientists (Eds.), *Southwest Indian Ridge lower crust and Moho. Proceed. Intern. ODP 360: 1-267*, <http://dx.doi.org/10.14379/iodp.proc.360.103.2017>.
- Maia M., Sichel S., Briais A. et al., 2016. Extreme mantle uplift and exhumation along a transpressive transform fault. *Nature Geosci.*, 9: 619-624, ISSN: 1752-0894, doi: 10.1038/NNGEO2759.
- Ohara Y., Yoshida T., Kato Y. and Kasuga S., 2001. Giant megamullion in the Parece Vela backarc basin. *Mar. Geophys. Res.*, 22: 47-61.
- Pushcharovsky Yu.M., Peyve A.A., Raznitsin Yu.N., Skolotnev S.G., Lapunov S.M and Tyrko N.N., 1988. Cape Verde fracture zone: rock composition and structures (Central Atlantic). *Geotectonika*, 6: 18-31 (in Russian).
- Pushcharovsky Yu.M., Raznitsin Yu.N., Mazarovich A.O., Skolotnev S.G., Kepezhinskas P.K., Tyrko N.N., Peyve A.A. and Dmitriev D.A., 1992. Fracture zones Arkhangelsky, Doldrums and Vernadsky in the Central Atlantic: structure and rocks composition. *Geotectonika*, 6: 63-79 (in Russian).
- Pushcharovsky Yu.M., Raznitsin Yu.N., Mazarovich A.O. et al., 1991. Structure of the Doldrums fracture zone Central Atlantic. *M. Nauka*, 224 pp. (in Russian).
- Sandwell D.T. and Smith W.H.F., 1997. Marine gravity anomaly from Geosat and ERS 1 satellite altimetry. *J. Geophys. Res.*, 102 (B5): 10039-10054.
- Sanfilippo A., Dick H.J.B., Marschall H.R., Lissenberg, C.J. and Urann B., 2018. Emplacement and high-temperature evolution of gabbros of the 16.5°N oceanic core complexes (Mid-Atlantic Ridge): Insights into the compositional variability of the lower oceanic crust. *Geochem. Geophys. Geosyst.*, 20, <https://doi.org/10.1029/2018GC007512>.
- Sclater J.G., Grindlay N.R., Madsen J.A. and Rommevaux-Jestin C., 2005. Tectonic interpretation of the Andrew Bain transform fault: Southwest Indian Ocean. *Geochem. Geophys. Geosyst.*, 6: Q09K10, doi:10.1029/2005GC000951.
- Schilling J.G. et al., 1995. Thermal structure of the mantle beneath the equatorial Mid-Atlantic Ridge-Inferences from the spatial variation of dredged basalt glass compositions. *J. Geophys. Res.*, 100: 10057-10076.

- Skolotnev S.G., Peyve A.A., Lavrushin V.Yu, Demidova T.A., Abramov S.S., Eskin A.E., Krinov D.I., Petrov V.V., Razdolina N.V., Turko N.N., Tsukanov N.V., Chaplygina N.L. and Sharikov E.V., 2006. Geological structure and indicators of hydrothermal ore-bearing activity at the junction of the southern rift segment and the Doldrums Transform Fracture Zone, Central Atlantic. *Dokl. Akad. Nauk*, 407 (3): 372-377.
- Smith D.K., Schouten H., Dick H.J.B. et al., 2014. Development and evolution of detachment faulting along 50 km of the Mid-Atlantic Ridge near 16.5°N. *Geochem. Geophys. Geosyst.*, 15: 4692-4710, <https://doi.org/10.1002/2014GC005563>.
- Stracke A. and Bourdon B., 2009. The importance of melt extraction for tracing mantle heterogeneity. *Geochim. Cosmochim. Acta*, 73 (1): 218-238, <https://doi.org/10.1016/j.gca.2008.10.015>.
- Teagle D.A.H., Alt J.C., Umino S. et al., 2006. *Proceed. IODP*, 309/312, doi: 10.2204/iodp.proc.309312.101.2006.
- Tucholke B.E., Behn M.D., Buck W.R. and Lin J. 2008. Role of melt supply in oceanic detachment faulting and formation of megamullions. *Geology*, 36 (6): 455-458, <https://doi.org/10.1130/G24639A.1>.
- Wernicke B., 1985. Uniform sense normal simple shear of the continental lithosphere. *Can. J. Earth Sci.*, 22: 108-125.
- White R.S., 1984. Atlantic oceanic crust: seismic structure of a slow-spreading ridge. *Geol. Soc. London Spec. Publ.*, 13: 101-111, <https://doi.org/10.1144/GSL.SP.1984.013.01.09>.
- Wilson J.T., 1965. A new class of faults and their bearing on continental drift. *Nature*, 207: 343-347.
- Woodcock N.H. and Fischer M. 1986. Strike-slip duplexes. *J. Struct. Geol.*, 8: 725-735.

Received, December 13, 2019

Accepted, January 8, 2020